HHS Public Access

Author manuscript

Toxicol Mech Methods. Author manuscript; available in PMC 2017 February 01.

Published in final edited form as:

Toxicol Mech Methods. 2016 February ; 26(2): 88–96. doi:10.3109/15376516.2015.1103000.

Connexin32: a mediator of acetaminophen-induced liver injury?

Michaël Maes[1], **Mitchell R. McGill**[2,#], **Tereza Cristina da Silva**[3], **Margitta Lebofsky**[2], **Cintia Maria Monteiro de Araújo**[3], **Taynã Tiburcio**[3], **Isabel Veloso Alves Pereira**[3], **Joost Willebrords**[1], **Sara Crespo Yanguas**[1], **Anwar Farhood**[4], **Maria Lucia Zaidan Dagli**[3], **Hartmut Jaeschke**[2], **Bruno Cogliati**[3,*], and **Mathieu Vinken**[1,*]

[1]Department of *In Vitro* Toxicology and Dermato-Cosmetology, Faculty of Medicine and Pharmacy, Vrije Universiteit Brussel, Brussels, Belgium.

[2]Department of Pharmacology, Toxicology and Therapeutics, University of Kansas Medical Center, Kansas City, Kansas, United States of America.

[3]Department of Pathology, School of Veterinary Medicine and Animal Science, University of São Paulo, São Paulo, Brazil.

[4]Department of Pathology, St. David's North Austin Medical Center, Austin, Texas, United States of America.

Abstract

Connexin32 is the building block of hepatocellular gap junctions, which control direct intercellular communication and thereby act as goalkeepers of liver homeostasis. This study was set up to investigate whether connexin32 is involved in hepatotoxicity induced by the analgesic and antipyretic drug acetaminophen. To this end, whole body connexin32 knock-out mice were overdosed with acetaminophen followed by sampling at different time points within a 24-hour time frame. Evaluation was done based upon a series of clinically and mechanistically relevant read-outs, including protein adduct formation, histopathological examination, measurement of alanine aminotransferase activity, cytokine production, levels of reduced and oxidized glutathione, and hepatic protein amounts of proliferating cell nuclear antigen. In essence, it was found that genetic ablation of connexin32 has no influence on several key events in acetaminophen-induced hepatotoxicity, including cell death, inflammation or oxidative stress, yet it does affect production of protein adducts as well as proliferating cell nuclear antigen steady-state protein levels. This outcome is not in line with previous studies, which are contradicting on their own, as both amplification and alleviation of this toxicological process by connexin32 have been described. This could question the suitability of the currently available models and tools to investigate the role of connexin32 in acetaminophen-triggered hepatotoxicity.

Contact information: Mathieu Vinken, Vrije Universiteit Brussel, Department of *In Vitro* Toxicology and Dermato-Cosmetology, Laarbeeklaan 103, B-1090 Brussels, Belgium; Tel: +32-2-4774587; Fax: +32-2-4774582; mvinken@vub.ac.be.

[#]Present address: Department of Pathology and Immunology, Washington University School of Medicine, St. Louis, Missouri, United States of America.

[*]These authors share equal seniorship.

Declaration of interest

The authors report no declarations of interest.

Keywords

connexin32; hepatotoxicity; acetaminophen; gap junction

1. Introduction

Connexin32 (Cx32) is major driver of cellular signaling in liver. As such, 6 Cx32 proteins assemble to form a hemichannel in a single hepatocyte, which then docks with an identical structure from a neighboring hepatocyte yielding a gap junction. The latter mediates the cell-to-cell transfer of small and hydrophilic compounds, such as second messengers (Vinken et al. 2008). This gap junctional intercellular communication (GJIC) is of paramount importance for various liver-specific functions, including xenobiotic biotransformation (Neveu et al. 1994; Shoda et al. 1999 and 2000). Compelling evidence now shows that hemichannels foresee an additional circuit for cellular communication independent of their role as building blocks of gap junctions. Unlike GJIC, hemichannel signaling occurs between the cytoplasm of individual cells and their extracellular environment. While gap junctions may be involved both in physiological and pathological processes, hemichannels seem to be consistently associated with the latter (Decrock et al. 2009; Maes et al. 2014; Vinken et al. 2010). In fact, connexin signaling has been causally linked to liver disease and toxicity (Vinken et al. 2009). Nonetheless, the exact role of Cx32-based communication in hepatotoxicity remains obscure. Administration of liver toxicants, including thioacetamide (Patel et al. 2012), *D*-galactosamine, carbon tetrachloride (Asamoto et al. 2004) and acetaminophen (APAP) (Naiki-Ito et al. 2010), to $Cx32^{-/-}$ C57BL/6 mice or Cx32-dominant negative transgenic Sprague-Dawley rats results in decreased serum aminotransferase levels as well as in less liver tissue damage compared to wild type (WT) animals. Likewise, ceramide synthase 2-null C57BL/6 mice, in which Cx32 is located in the cytosol of hepatocytes and that display aberrant GJIC, are less susceptible to APAP-induced hepatotoxicity (Park et al. 2013). This suggests a role for Cx32-based gap junctions in the dissemination of damage signals. In contrast, another report described increased serum aminotransferase values and more pronounced liver insults in $Cx32^{-/-}$ C57BL/6 mice after administration of APAP, indicating a cytoprotective function for hepatic Cx32 in APAP-induced injury (Igarashi et al. 2014). There are substantial differences in the set-up of these studies, especially those using APAP, and with some exceptions (Igarashi et al. 2014), they have mainly focused on the measurement of parameters of cell death, which indeed is the most typical read-out of liver toxicity. However, like for most other hepatotoxicants, this ultimate outcome of APAP poisoning is preceded by a number of key events in which Cx32 signaling could also play a role. Therefore, in the present study, Cx32-deficient mice were overdosed with APAP followed by evaluation of a number of mechanistically relevant parameters indicative of important steps in the occurrence of this common kind of drug-induced liver toxicity.

2. Methods

Generation and genotypic control of Cx32 deficient mice

Male WT C57BL/6 mice were obtained from Jackson Laboratories (USA). $Cx32^{-/-}$ mice were kindly provided by Dr. Klaus Willecke, which were generated by disrupting the Cx32 coding region in the mouse genome through insertion of a selectable gene that codes for neomycin resistance *via* homologous recombination (Nelles et al. 1996). These animals were backcrossed with WT C57BL/6 mice. Genotype was controlled by polymerase chain reaction (PCR) analysis of DNA from mouse tail tips as previously described (Evert et al. 2002; Moennikes et al. 1999). Briefly, mice tails tips were digested in 20 mg/ml proteinase K solution (Invitrogen, USA) at 65°C during 2 hours. DNA was precipitated with sodium acetate and ethanol. Pellets were washed in ethanol and resuspended in Tris-buffered saline (*i.e.* 20 mM Tris and 0.15 M NaCl) containing ethylenediaminetetraacetic acid. Primers used for detection of the Cx32 WT allele were 5'-CCATAAGTCAGGTGTAAAGGAGC-3' and 5'-AGATAAGCTGCAGGGACCATAGG-3', generating a PCR product of 550 base pairs. Primer pairs used for detection of the Cx32-defective allele were 5'-CCATAAGTCAGGTGTAAAGGAGC-3' and 5'-ATCATGCGAAACGATCCTCATCC-3', generating a PCR product of 414 base pairs. Standard PCR amplifications were carried out using SuperMix (Invitrogen, USA), 10 pmol of each PCR amplification primer and 100 ng of template DNA in 25 μl reaction volume. Samples were denatured for 2 minutes at 94°C followed by 34 cycles of 94°C for 30 seconds, 60°C for 1 minute, 72°C for 1 minute and finally 72°C for 4 minutes. The amplicons were loaded onto agarose gel in Tris-buffered saline. The gel was visualized by BlueGreen Dye (LGC Biotechnologia, Brazil) according to the manufacturer's instructions. Analyses were performed using ImageQuant LAS 400 (GE Healthcare Life Sciences, USA).

Animal treatment

Animals were housed in the animal facility of the School of Veterinary Medicine and Animal Science of the University of São Paulo, Brazil. Mice were kept in a room with ventilation (*i.e.* 16-18 air changes/hour), relative humidity (*i.e.* 45-65%), controlled temperature (*i.e.* 20-24°C) and light/dark cycle 12:12 and were given water and balanced diet (NUVILAB-CR1, Nuvital Nutrientes LTDA, Brazil) *ad libitum*. Different conditions for induction of liver injury with APAP were tested in preliminary experiments, including dose (*i.e.* 100-500 mg/kg body weight) and way of administration (*i.e.* oral gavage, intravenous and intraperitoneal injection). In the optimized setting, mice were starved 15-16 hours *prior* to APAP administration. APAP (Sigma-Aldrich, USA) was dissolved in saline, slightly heated and injected (*i.e.* 30-37°C) intraperitoneally at 300 mg/kg body weight after which animals regained free access to food. Mice were euthanized at the start of the experiment and 1, 6 and 24 hours after APAP injection by exsanguination during sampling under isoflurane-induced anesthesia. Blood, collected by cardiac puncture, was drawn into a heparinized syringe and centrifuged for 10 minutes at 1503x*g*, and serum was stored at −20°C. Livers were excised and fragments were fixed in 10% phosphate-buffered formalin or snap-frozen in liquid nitrogen with storage at −80°C. This study has been approved by the Committee on Bioethics of the School of Veterinary Medicine and Animal Science of the University of São Paulo, Brazil (protocol number 9999100314) and all animals received

humane care according to the criteria outlined in the “Guide for the Care and Use of Laboratory Animals”.

Analysis of hepatic protein adducts

APAP-protein adducts were measured by high-pressure liquid chromatography with electrochemical detection as previously described (Muldrew et al. 2002) with modifications (McGill et al. 2013). Briefly, protein samples were filtered through size exclusion columns *prior* to digestion with proteases and the protein-derived APAP-cysteine (APAP-CYS) conjugates were quantified and normalized to sample protein concentration in the original samples.

Histopathological liver examination

For microscopic evaluation, formalin-fixed liver fragments were embedded in paraffin and 5 μm sections were stained with hematoxylin-eosin for blinded evaluation of liver damage as described elsewhere (Gujral et al. 2002). The percent of cell death was estimated by evaluating the number of microscopic fields with necrosis compared to the cross-sectional areas. Pictures were taken at 100x magnification using a light microscope (Carl Zeiss, USA).

Analysis of serum alanine aminotransferase

Alanine aminotransferase (ALT) was measured with an automated spectrophotometric Labmax 240 analyzer (Labtest Diagnostica, Brazil) after appropriate dilution of serum samples. Values were expresses in IU/L.

Analysis of liver and serum cytokines

Liver tissue was homogenized in lysis buffer with protease inhibitors (Roche, Germany). Homogenates were centrifuged at 14000x*g* for 15 minutes at 4°C and protein concentrations in supernatants were determined according to the Bradford procedure (Bradford 1976) using a commercial kit (Bio-Rad, USA) with bovine serum albumin as a standard. Enzyme-linked immunosorbent assay (ELISA) kits were used to measure levels of mouse interleukin (IL)-1β, IL-6, IL-10, interferon γ (IFNγ) and tumor necrosis factor α (TNFα) (BD Biosciences, USA). Wells of a 96-well plate were coated overnight with appropriate monoclonal antibody diluted in coating buffer and blocked for 1 hour with phosphate-buffered saline containing fetal bovine serum. Subsequently, wells were incubated with liver homogenate, diluted serum or standard solution for 2 hours, followed by incubation with appropriate biotinylated monoclonal antibody and streptavidin-horseradish peroxidase conjugate for 1 hour and 30 minutes, respectively. Finally, wells were exposed to tetramethylbenzidine substrate reagent for 30 minutes. The reaction was stopped by adding phosphoric acid and absorbance was measured at 450 nm with wavelength correction at 570 nm using a Varioskan™ Flash Multimode Reader (Thermo Scientific, USA).

Hepatic glutathione and glutathione disulfide analysis

Reduced glutathione (GSH) and oxidized glutathione disulfide (GSSG) levels in liver tissue were measured using a modified Tietze assay (Jaeschke and Mitchell 1990). Briefly, frozen liver tissue was homogenized in sulfosalicylic acid/ethylenediaminetetraacetic acid and

centrifuged at 18000x*g* for 5 minutes at 4°C to remove precipitated proteins. After further dilution with potassium phosphate buffer, samples were assayed with a cycling reaction utilizing GSH reductase and dithionitrobenzoic acid. Measurement of GSSG was performed using the same method after trapping GSH with *N*-ethylmaleimide and removal by solid phase extraction (Jaeschke and Mitchell 1990).

Analysis of hepatic proliferating cell nuclear antigen

Protein expression of proliferating cell nuclear antigen (PCNA) was studied by means of immunoblotting as previously described (Bajt et al. 2000). Briefly, liver tissue was homogenized in 25 mM 4-(2-hydroxyethyl)-1-piperazineethanesulfonic acid buffer containing 5 mM ethylendiaminetetraacetic acid, 2 mM dithiothreitol, 1% 3-[(3-cholamidopropyl)dimethylammonio]propanesulfonate and 1 μg/ml pepstatin, leupeptin and aprotinin. Homogenates were centrifuged at 14000x*g* for 5 minutes at 4°C. Protein concentrations in supernatants were determined using a commercial bicinchoninic acid kit (Pierce Biotechnology, USA). Protein lysates (*i.e.* 50 μg per lane) were resolved on 4-20% sodium dodecyl sulphate polyacrylamide gel electrophoresis under reducing conditions. Separated proteins were transferred to polyvinylidine difluoride membranes (Millipore Corporation, USA) and blocked overnight at 4°C with 5% milk in Tris-buffered saline containing 0.1% Tween-20 and 0.1% bovine serum albumin. After washing with Tris-buffered saline, membranes were incubated with a mouse monoclonal anti-PCNA antibody (Santa Cruz Biotechnology, USA) for 2 hours at room temperature. Membranes were washed and incubated with the appropriate secondary horseradish peroxidase-coupled antibody (Santa Cruz Biotechnology, USA) for 1 hour at room temperature. Proteins were visualized by enhanced chemiluminescence (Amersham Biosciences, USA) according to the manufacturer's instructions. Densitometric analysis was performed with a GS170 Calibrated Imaging Densitometer (Bio-Rad, USA) using Quantity One 4.0.3 software (Bio-Rad, USA). For semi-quantification purposes, PCNA signals were normalized against β-actin signals and expressed as relative alterations compared to WT animals.

Statistical analysis

The number of repeats (n) for each analysis varied and is specified in the discussion of the results. All data were expressed as mean ± standard error of the mean (SEM). Results were statistically processed by 1-way analysis of variance (ANOVA) followed by *post hoc* tests with Bonferroni correction or 2-tailed unpaired student *t*-tests and Welch's correction using GraphPad Prism6 software with probability (*p*) values of less than or equal to 0.05 considered as significant.

3. Results

Effect of Cx32 deficiency on hepatic protein adduct formation

Whole body $Cx32^{-/-}$ mice were used in order to investigate whether Cx32 is involved in APAP toxicity. Genotyping indeed showed the absence of the WT Cx32 transcript in these animals (Figure 1). WT and $Cx32^{-/-}$ mice were overdosed with APAP followed by sampling at different time points. APAP-induced hepatotoxicity depends on biotransformation mediated by cytochrome P450 2E1, yielding the deleterious metabolite *N*-acetyl-*p*-

benzoquinone imine (NAPQI) (Dahlin et al. 1984). Under normal circumstances, NAPQI can be rapidly detoxified by binding to GSH. However, in case of APAP overdosing, GSH becomes depleted and NAPQI can react with protein sulfhydryl groups, which leads to the formation of noxious liver protein adducts (Mitchell et al. 1973). In this respect, APAP-protein adducts were readily detectable in all mice already 1 hour after APAP administration. At 6 hours, a significant ($p \leq 0.05$) lower number of APAP-protein adducts was observed in $Cx32^{-/-}$ mice compared to WT animals (Figure 2).

Effect of Cx32 deficiency on hepatic cell death

The formation of APAP-protein adducts in APAP toxicity ultimately burgeons into the onset of massive hepatocyte cell death, which typically occurs in a zonated pattern. Specifically, necrotic patches appear around the central vein, where expression of cytochrome P450 enzymes responsible for NAPQI formation is highest (Lee et al. 1996). Histopathological analysis did not reveal any liver injury 1 hour after APAP overdosing (data not shown). Necrotic areas became detectable microscopically 6 hours after administration of APAP to WT animals (Figure 3A). Despite a lower amount of APAP-protein adducts in $Cx32^{-/-}$ mice after 6 hours (Figure 2), quantification of the cell death areas revealed no major differences in $Cx32^{-/-}$ mice compared to WT animals after 6 and 24 hours (Figure 3B). This was reflected at the biochemical level by measurement of serum levels of ALT (Figure 3C). This cytosolic enzyme leaks from the cell into the serum upon membrane damage, which occurs in the case of necrosis (McGill and Jaeschke 2014). In all animals tested, ALT levels were elevated starting 6 hours after APAP administration and decreased towards 24 hours (Figure 3C).

Effects of Cx32 deficiency on hepatic inflammation

APAP overdosing activates the inflammatory machinery, which partly relies on nonparenchymal liver cells and that is associated with the formation of a plethora of pro-inflammatory and anti-inflammatory cytokines (Blazka et al. 1995). However, in this study, only subtle changes in hepatic levels of the prototypical pro-inflammatory cytokines IL-1β and TNFα were recorded in the 24-hour timeframe following APAP administration to WT animals (43). Hepatic IL-1β amounts of $Cx32^{-/-}$ animals were significantly ($p \leq 0.05$) lower at the start of the experiment and after 6 hours (Figure 4). These effects were only seen in liver and not in serum, where IL-1β and TNFα levels were below the detection limit for both study groups at the start of APAP administration and after 1 hour. Liver profiles of IL-6 were similar in all animals, with a prominent peak 1 day posttreatment and no differences between the 2 test groups (Figure 4). No differences were detected in serum quantities of IL-6. Anti-inflammatory IL-10 tended to progressively increase in livers of all animals 6 hours after APAP overdosing, followed by a decline at 24 hours in WT animals, which was less ($p \leq 0.05$) pronounced in $Cx32^{-/-}$ mice. IL-10 behaved in the opposite way in serum, with an increase from 6 to 24 hours following APAP treatment in all conditions. Serum levels of IFNγ were below the detection limit. Significantly ($p \leq 0.05$) lower levels of IFNγ were noticed at 6 hours in $Cx32^{-/-}$ animals compared to WT mice (Figure 4).

Effects of Cx32 deficiency on hepatic oxidative stress

Several mechanisms underlie oxidative stress associated with APAP toxicity, with a crucial one being GSH depletion due to excessive NAPQI production (Jaeschke 1990; Knight et al. 2001). In this study, a reduction in the GSH pool indeed became evident 1 hour after APAP overdosing of all mice. This was followed by a recovery at 24 hours (Figure 5A). GSH acts as an anti-oxidant and is converted to its oxidized GSSG form upon reaction with reactive oxygen species. For all experimental groups, GSSG formation peaked 24 hours after APAP administration, which was significantly ($p \leq 0.05$) lower in $Cx32^{-/-}$ mice (Figure 5B). However, there were no differences in GSSG/GSH ratios (Figure 5C), suggesting equal occurrence of oxidative stress in all test groups.

Effects of Cx32 deficiency on hepatic regeneration

Upon insult, such as in APAP toxicity, the liver typically initiates a well-coordinated regenerative response to repair damaged tissue. Proliferating hepatocytes adjacent to necrotic areas thereby replace dead counterparts (Mehendale 2005). Dividing cells abundantly produce PCNA, a co-factor of DNA polymerase necessary for DNA synthesis and repair (Theocharis et al. 1994). Accordingly, PCNA expression is commonly used as an indicator of regenerative activity in hepatic tissue following injury (Bajt et al. 2003; Xie et al. 2015). Hepatic PCNA protein amounts were significantly ($p \leq 0.01$) higher in $Cx32^{-/-}$ mice compared to WT animals at 24 hours (Figure 6), suggesting that Cx32 might influence the regeneration process after APAP-induced injury.

4. Discussion

Drug-induced liver injury accounts for more than 50% of all clinical cases of acute liver failure, with the vast majority being caused by overdosing with the readily available analgesic and antipyretic drug APAP (Ichai and Samuel 2011). Several signaling cascades are known to underlie APAP-induced liver toxicity, yet little is known about the involvement of GJIC. A limited number of reports have described a role for Cx32-based gap junctions in APAP-triggered hepatotoxicity using genetically modified animals, albeit with contradicting outcome (Igarashi et al. 2014; Naiki-Ito et al. 2010). In this respect, Naiki-Ito and colleagues administered up 1000 mg/kg APAP intragastrically to rats carrying a mutated Cx32 gene and noticed decreased ALT serum levels and lowered histopathological damage after 24 hours (Naiki-Ito et al. 2010). By contrast, in the study of Igarashi and group, whole body Cx32 knock-out mice were used with sampling after 1 hour and 1 day. At 100 and 200 mg/kg APAP injected intraperitoneally, increased ALT quantities and more pronounced necrotic cell death were observed in $Cx32^{-/-}$ animals. These effects were, however, not seen at 300 kg/mg APAP (Igarashi et al. 2014), a commonly used dose for experimental testing purposes (Harril et al. 2009; McGill et al. 2012; Mossanen and Tacke 2015), which is in line with the findings of our study. With the exception of a lower hepatic amount of IL-1β after 0 and 6 hours and rather fortuitous variations in IL-10 and IFNγ amounts at a single time point, we also failed to detect modifications in serum and liver pro-inflammatory and anti-inflammatory cytokine levels in Cx32-deficient mice. This equally holds true for the GSSG/GSH ratios. Regarding the latter, Igarashi and group found less decreased GSH and GSSG levels in APAP-treated Cx32 knock-out mice and attributed the protective effect of

Cx32 against liver injury to changes in GSH transmission between hepatocytes (Igarashi et al. 2014). GSH indeed is known to permeate gap junctions and it has been reported that hemichannels, including those based on Cx32, can also transport GSH (Rana and Dringen 2007; Tong et al. 2015). At the more upstream mechanistic platform of APAP toxicity, cell death results from protein adduct formation involving NAPQI. We found that this process was less manifested in $Cx32^{-/-}$ mice, which could indicate a lower metabolic activity upon genetic ablation of Cx32. However, Patel and coworkers showed that the activity of cytochrome P450 2E1, which catalyzes NAPQI formation, is not altered in $Cx32^{-/-}$ mice (Patel et al., 2012). Although delayed liver regeneration has been described for Cx32-deficient mice (Dagli et al. 2004), higher hepatic amounts of PCNA were found in $Cx32^{-/-}$ mice after APAP-induced liver injury. Collectively, these data thus suggest that Cx32 does not affect cell death, inflammation or oxidative stress, all which are major hallmarks of APAP-induced liver toxicity. Despite some similarities, there are several discrepancies between these results and the findings of Naiki-Ito and colleagues, and Igarashi and group (Igarashi et al. 2014; Naiki-Ito et al. 2010). This is likely to be due to differences in experimental set-up, including animal species, dose and route of administration of APAP. A number of questions can be raised about the model that was used in these studies. Indeed, genetic deletion of genes as such, *in casu* Cx32, may trigger off-target effects. In this respect, given its key function in liver homeostasis (Vinken et al. 2008), ablation of Cx32 could cause stress, which in turn may activate compensatory mechanisms, such as those related to oxidative stress, that increase defense and hence modify susceptibility to APAP-induced toxicity. In this light, Cx32-deficient mice are known to display increase susceptibility to both spontaneous and chemically induced liver tumors (Temme et al. 1997). It should also be mentioned that the models used, in particular whole body Cx32 knock-out animals, do not allow to distinguish between Cx32-based GJIC and Cx32-related hemichannel signaling. Connexin hemichannels have been considered merely as structural precursors of gap junctions for a long time. In the last decade, it has become clear that they provide a pathway for communication on their own, albeit between the cytoplasm of individual cells and their extracellular environment, and not between 2 neighboring cells as is the case for gap junctions. Unlike the latter, hemichannels tend to specifically open up in pathological conditions (Decrock et al. 2009; Maes et al. 2014; Vinken et al. 2010). In this context, our group previously reported that Cx32-based hemichannels, but not their full channel counterparts, facilitate cell death in primary hepatocyte cultures (Vinken et al. 2010). Although this scenario may also take place during APAP-induced liver toxicity *in vivo*, it cannot be captured with the currently available animal models, as they are devoid of Cx32 protein, being the common building block of hepatocellular gap junctions and hemichannels. In the past few years, mouse models with specific modification of hemichannel activity have been developed for connexins other than Cx32, including Cx43 (Dobrowolski et al. 2008). It can be expected that upon introduction of such models for Cx32, more light will be shed onto its actual role in APAP-induced liver toxicity.

5. Conclusion

It was found that Cx32 ablation has no influence on several key events in APAP-induced hepatotoxicity, including cell death, inflammation or oxidative stress, yet this genetic

modification does affect production of protein adducts and PCNA steady-state protein levels. This outcome is not in line with previous studies, which are contradicting on their own, as both amplification and alleviation of this toxicological process by Cx32 have been described. This could question the suitability of the currently available models and tools to investigate the role of Cx32 in APAP-triggered hepatotoxicity.

Acknowledgments

The authors wish to thank Miss Tineke Vanhalewyn, Miss Dinja De Win, Miss Shirlei Meire da Silva and Mister José Alexandre Coelho Pimentel for their dedicated technical assistance. This work was financially supported by grants from the Agency for Innovation by Science and Technology in Flanders (IWT), the European Research Council (ERC Starting Grant 335476), the Fund for Scientific Research-Flanders (FWO grants G009514N and G010214N), the University Hospital of the Vrije Universiteit Brussel-Belgium ("Willy Gepts Fonds" UZ-VUB), the US National Institutes of Health (R01 DK102142), the University of São Paulo-Brazil and the Foundation for Research Support of the State of São Paulo-Brazil (FAPESP SPEC grant 2013/50420-6).

List of abbreviations

ALT	alanine aminotransferase
ANOVA	analysis of variance
APAP	acetaminophen
APAP-CYS	APAP-cysteine
Cx	connexin
ELISA	enzyme-linked immunosorbent assay
GJIC	gap junctional intercellular communication
GSH	(reduced) glutathione
GSSG	(oxidized) glutathione disulfide
IFNγ	interferon γ
IL-1β/6/10	interleukin 1β/6/10
n	number of repeats
NAPQI	*N*-acetyl-*p*-benzoquinone imine
p	probability
PCNA	proliferating cell nuclear antigen
PCR	polymerase chain reaction
SEM	standard error of the mean
TNFα	tumor necrosis factor α
WT	wild type

References

Asamoto M, Hokaiwado N, Murasaki T, Shirai T. Connexin 32 dominant-negative mutant transgenic rats are resistant to hepatic damage by chemicals. Hepatology. 2004; 40:205–210. [PubMed: 15239104]

Bajt ML, Knight TR, Farhood A, Jaeschke H. Scavenging peroxynitrite with glutathione promotes regeneration and enhances survival during acetaminophen-induced liver injury in mice. J Pharmacol Exp Ther. 2003; 307:67–73. [PubMed: 12954812]

Bajt ML, Lawson JA, Vonderfecht SL, Gujral JS, Jaeschke H. Protection against Fas receptor-mediated apoptosis in hepatocytes and nonparenchymal cells by a caspase-8 inhibitor in vivo: evidence for a postmitochondrial processing of caspase-8. Toxicol Sci. 2000; 58:109–117. [PubMed: 11053547]

Blazka ME, Wilmer JL, Holladay SD, Wilson RE, Luster MI. Role of proinflammatory cytokines in acetaminophen hepatotoxicity. Toxicol Appl Pharmacol. 1995; 133:43–52. [PubMed: 7597709]

Bradford MM. A rapid and sensitive method for the quantitation of microgram quantities of protein utilizing the principle of protein-dye binding. Anal Biochem. 1976; 72:248–254. [PubMed: 942051]

Dagli ML, Yamasaki H, Krutovskikh V, Omori Y. Delayed liver regeneration and increased susceptibility to chemical hepatocarcinogenesis in transgenic mice expressing a dominant-negative mutant of connexin32 only in the liver. Carcinogenesis. 2004; 25:483–492. [PubMed: 14688024]

Dahlin DC, Miwa GT, Lu AY, Nelson SD. N-acetyl-p-benzoquinone imine: a cytochrome P-450-mediated oxidation product of acetaminophen. Proc Natl Acad Sci U S A. 1984; 81:1327–1331. [PubMed: 6424115]

Decrock E, Vinken M, De Vuyst E, Krysko DV, D'Herde K, Vanhaecke T, Vandenabeele P, Rogiers V, Leybaert L. Connexin-related signaling in cell death: to live or let die? Cell Death Differ. 2009; 16:524–536. [PubMed: 19197295]

Dobrowolski R, Sasse P, Schrickel JW, Watkins M, Kim JS, Rackauskas M, Troatz C, Ghanem A, Tiemann K, Degen J, Bukauskas FF, Civitelli R, Lewalter T, Fleischmann BK, Willecke K. The conditional connexin43G138R mouse mutant represents a new model of hereditary oculodentodigital dysplasia in humans. Hum Mol Genet. 2008; 17:539–554. [PubMed: 18003637]

Evert M, Ott T, Temme A, Willecke K, Dombrowski F. Morphology and morphometric investigation of hepatocellular preneoplastic lesions and neoplasms in connexin32-deficient mice. Carcinogenesis. 2002; 23:697–703. [PubMed: 12016140]

Gujral JS, Knight TR, Farhood A, Bajt ML, Jaeschke H. Mode of cell death after acetaminophen overdose in mice: apoptosis or oncotic necrosis? Toxicol Sci. 2002; 67:322–328. [PubMed: 12011492]

Harrill AH, Ross PK, Gatti DM, Threadgill DW, Rusyn I. Population-based discovery of toxicogenomics biomarkers for hepatotoxicity using a laboratory strain diversity panel. Toxicol Sci. 2009; 110:235–243. [PubMed: 19420014]

Ichai P, Samuel D. Epidemiology of liver failure. Clin Res Hepatol Gastroenterol. 2011; 35:610–617. [PubMed: 21550329]

Igarashi I, Maejima T, Kai K, Arakawa S, Teranishi M, Sanbuissho A. Role of connexin 32 in acetaminophen toxicity in a knockout mice model. Exp Toxicol Pathol. 2014; 66:103–110. [PubMed: 24263089]

Jaeschke H. Glutathione disulfide formation and oxidant stress during acetaminophen-induced hepatotoxicity in mice in vivo: the protective effect of allopurinol. J Pharmacol Exp Ther. 1990; 255:935–941. [PubMed: 2262912]

Jaeschke H, Mitchell JR. Use of isolated perfused organs in hypoxia and ischemia/reperfusion oxidant stress. Methods Enzymol. 1990; 186:752–759. [PubMed: 2233332]

Knight TR, Kurtz A, Bajt ML, Hinson JA, Jaeschke H. Vascular and hepatocellular peroxynitrite formation during acetaminophen toxicity: role of mitochondrial oxidant stress. Toxicol Sci. 2001; 62:212–220. [PubMed: 11452133]

Lee SS, Buters JT, Pineau T, Fernandez-Salguero P, Gonzalez FJ. Role of CYP2E1 in the hepatotoxicity of acetaminophen. J Biol Chem. 1996; 271:12063–12067. [PubMed: 8662637]

Maes M, Decrock E, Cogliati B, Oliveira AG, Marques PE, Dagli ML, Menezes GB, Mennecier G, Leybaert L, Vanhaecke T, Rogiers V, Vinken M. Connexin and pannexin (hemi)channels in the liver. Front Physiol. 2014; 4:405. [PubMed: 24454290]

McGill MR, Jaeschke H. Mechanistic biomarkers in acetaminophen-induced hepatotoxicity and acute liver failure: from preclinical models to patients. Expert Opin Drug Metabol Toxicol. 2014; 10:1005–1017.

McGill MR, Lebofsky M, Norris HRK, Slawson MH, Bajt ML, Xie YC, Williams CD, Wilkins DG, Rollins DE, Jaeschke H. Plasma and liver acetaminophen-protein adduct levels in mice after acetaminophen treatment: Dose-response, mechanisms, and clinical implications. Toxicol Appl Pharmacol. 2013; 269:240–249. [PubMed: 23571099]

McGill MR, Williams CD, Xie Y, Ramachandran A, Jaeschke H. Acetaminophen-induced liver injury in rats and mice: comparison of protein adducts, mitochondrial dysfunction, and oxidative stress in the mechanism of toxicity. Toxicol Appl Pharmacol. 2012; 264:387–394. [PubMed: 22980195]

Mehendale HM. Tissue repair: an important determinant of final outcome of toxicant-induced injury. Toxicol Pathol. 2005; 33:41–51. [PubMed: 15805055]

Mitchell JR, Jollow DJ, Potter WZ, Gillette JR, Brodie BB. Acetaminophen-induced hepatic necrosis. IV. Protective role of glutathione. J Pharmacol Exp Ther. 1973; 187:211–217. [PubMed: 4746329]

Moennikes O, Buchmann A, Ott T, Willecke1 K, Schwarz M. The effect of connexin32 null mutation on hepatocarcinogenesis in different mouse strains. Carcinogenesis. 1999; 20:1379–1382. [PubMed: 10383916]

Mossanen JC, Tacke F. Acetaminophen-induced acute liver injury in mice. Lab Anim. 2015; 49:30–36. [PubMed: 25835736]

Muldrew KL, James LP, Coop L, McCullough SS, Hendrickson HP, Hinson JA, Mayeux PR. Determination of acetaminophen-protein adducts in mouse liver and serum and human serum after hepatotoxic doses of acetaminophen using high-performance liquid chromatography with electrochemical detection. Drug Metabol Dispos. 2002; 30:446–451.

Naiki-Ito A, Asamoto M, Naiki T, Ogawa K, Takahashi S, Sato S, Shirai T. Gap junction dysfunction reduces acetaminophen hepatotoxicity with impact on apoptotic signaling and connexin 43 protein induction in rat. Toxicol Pathol. 2010; 38:280–286. [PubMed: 20097795]

Nelles E, Butzler C, Jung D, Temme A, Gabriel HD, Dahl U, Traub O, Stumpel F, Jungermann K, Zielasek J, Toyka KV, Dermietzel R, Willecke K. Defective propagation of signals generated by sympathetic nerve stimulation in the liver of connexin32-deficient mice. Proc Natl Acad Sci U S A. 1996; 93:9565–9570. [PubMed: 8790370]

Neveu MJ, Babcock KL, Hertzberg EL, Paul DL, Nicholson BJ, Pitot HC. Colocalized alterations in connexin32 and cytochrome P450IIB1/2 by phenobarbital and related liver tumor promoters. Cancer Res. 1994; 54:3145–3152. [PubMed: 8205533]

Park WJ, Park JW, Erez-Roman R, Kogot-Levin A, Bame JR, Tirosh B, Saada A, Merrill AH, Pewzner-Jung Y, Futerman AH. Protection of a ceramide synthase 2 null mouse from drug-induced liver injury: role of gap junction dysfunction and connexin 32 mislocalization. J Biol Chem. 2013; 288:30904–30916. [PubMed: 24019516]

Patel SJ, Milwid JM, King KR, Bohr S, Iracheta-Velle A, Li M, Vitalo A, Parekkadan B, Jindal R, Yarmush ML. Gap junction inhibition prevents drug-induced liver toxicity and fulminant hepatic failure. Nat Biotechnol. 2012; 30:179–183. [PubMed: 22252509]

Rana S, Dringen R. Gap junction hemichannel-mediated release of glutathione from cultured rat astrocytes. Neurosci Lett. 2007; 415:45–48. [PubMed: 17222973]

Shoda T, Mitsumori K, Onodera H, Toyoda K, Uneyama C, Imazawa T, Hirose M. The relationship between decrease in Cx32 and induction of P450 isozymes in the early phase of clofibrate hepatocarcinogenesis in the rat. Arch Toxicol. 1999; 73:373–380. [PubMed: 10550479]

Shoda T, Mitsumori K, Onodera H, Toyoda K, Uneyama C, Takada K, Hirose M. Liver tumor-promoting effect of beta-naphthoflavone, a strong CYP 1A1/2 inducer, and the relationship between CYP 1A1/2 induction and Cx32 decrease in its hepatocarcinogenesis in the rat. Toxicol Pathol. 2000; 28:540–547. [PubMed: 10930040]

Temme A, Buchmann A, Gabriel HD, Nelles E, Schwarz M, Willecke K. High incidence of spontaneous and chemically induced liver tumors in mice deficient for connexin32. Curr Biol. 1997; 7:713–716. [PubMed: 9285723]

Theocharis SE, Skopelitou AS, Margeli AP, Pavlaki KJ, Kittas C. Proliferating cell nuclear antigen expression in regenerating rat liver after partial hepatectomy. Dig Dis Sci. 1994; 39:245–252. [PubMed: 7906221]

Tong X, Lopez W, Ramachandran J, Ayad WA, Liu Y, Lopez-Rodriguez A, Harris AL, Contreras JE. Glutathione release through connexin hemichannels: Implications for chemical modification of pores permeable to large molecules. J Gen Physiol. 2015; 146:245–254. [PubMed: 26324677]

Vinken M, Decrock E, De Vuyst E, De Bock M, Vandenbroucke RE, De Geest BG, Demeester J, Sanders NN, Vanhaecke T, Leybaert L, Rogiers V. Connexin32 hemichannels contribute to the apoptotic-to-necrotic transition during Fas-mediated hepatocyte cell death. Cell Mol Life Sci. 2010; 67:907–918. [PubMed: 19960225]

Vinken M, Doktorova T, Decrock E, Leybaert L, Vanhaecke T, Rogiers V. Gap junctional intercellular communication as a target for liver toxicity and carcinogenicity. Crit Rev Biochem Mol Biol. 2009; 44:201–222. [PubMed: 19635038]

Vinken M, Henkens T, De Rop E, Fraczek J, Vanhaecke T, Rogiers V. Biology and pathobiology of gap junctional channels in hepatocytes. Hepatology. 2008; 47:1077–1088. [PubMed: 18058951]

Xie Y, Ramachandran A, Breckenridge DG, Liles JT, Lebofsky M, Farhood A, Jaeschke H. Inhibitor of apoptosis signal-regulating kinase 1 protects against acetaminophen-induced liver injury. Toxicol Appl Pharmacol. 2015; 286:1–9. [PubMed: 25818599]

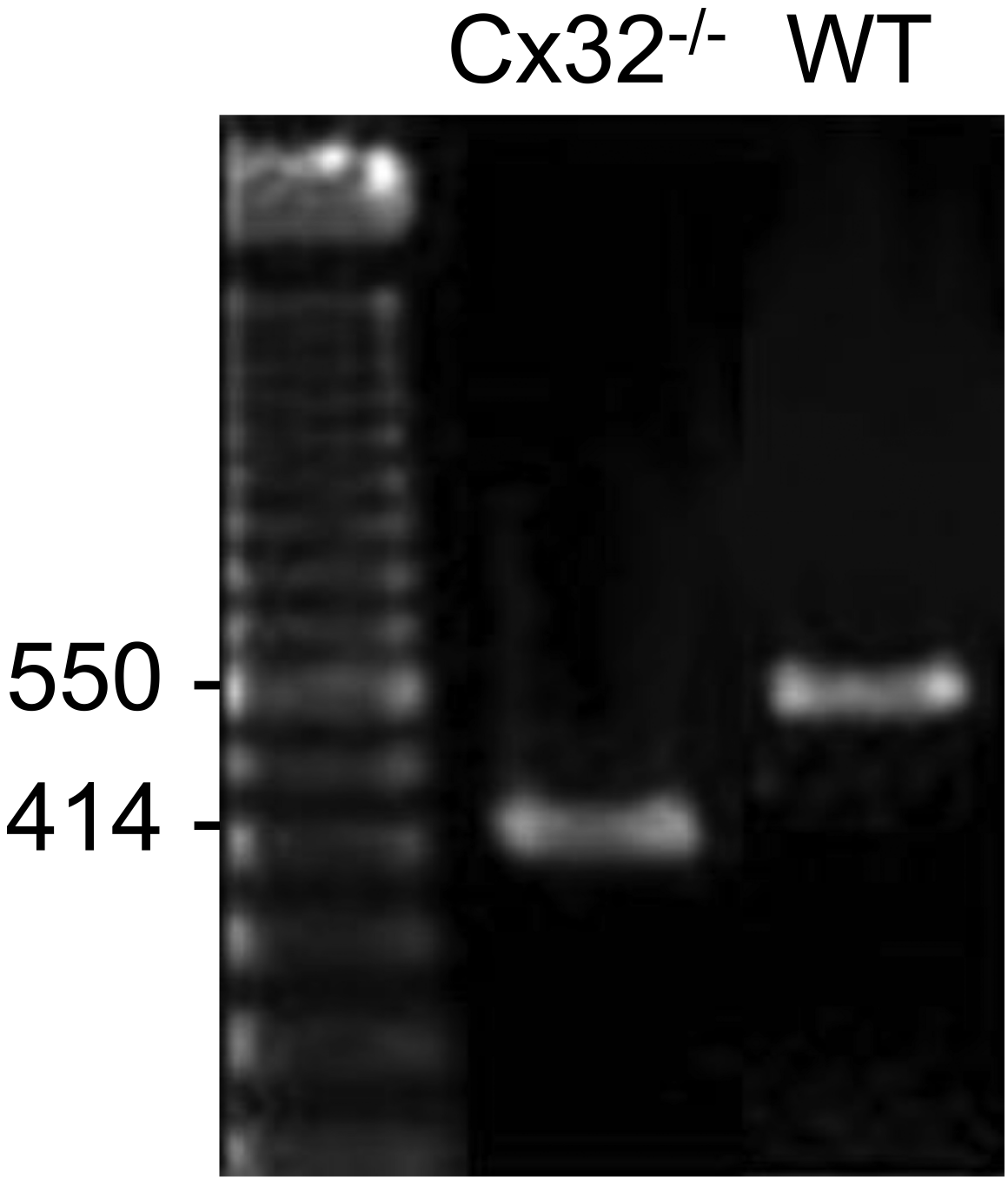

Figure 1. Genotypic control of Cx32-deficient mice

DNA was extracted from mouse tail tips and subjected to PCR using primer pairs specific for the Cx32 WT allele, generating a PCR product of 550 base pairs, or the Cx32-defective allele, generating a PCR product of 414 base pairs. Samples were loaded on agarose gel and visualized with BlueGreen Dye.

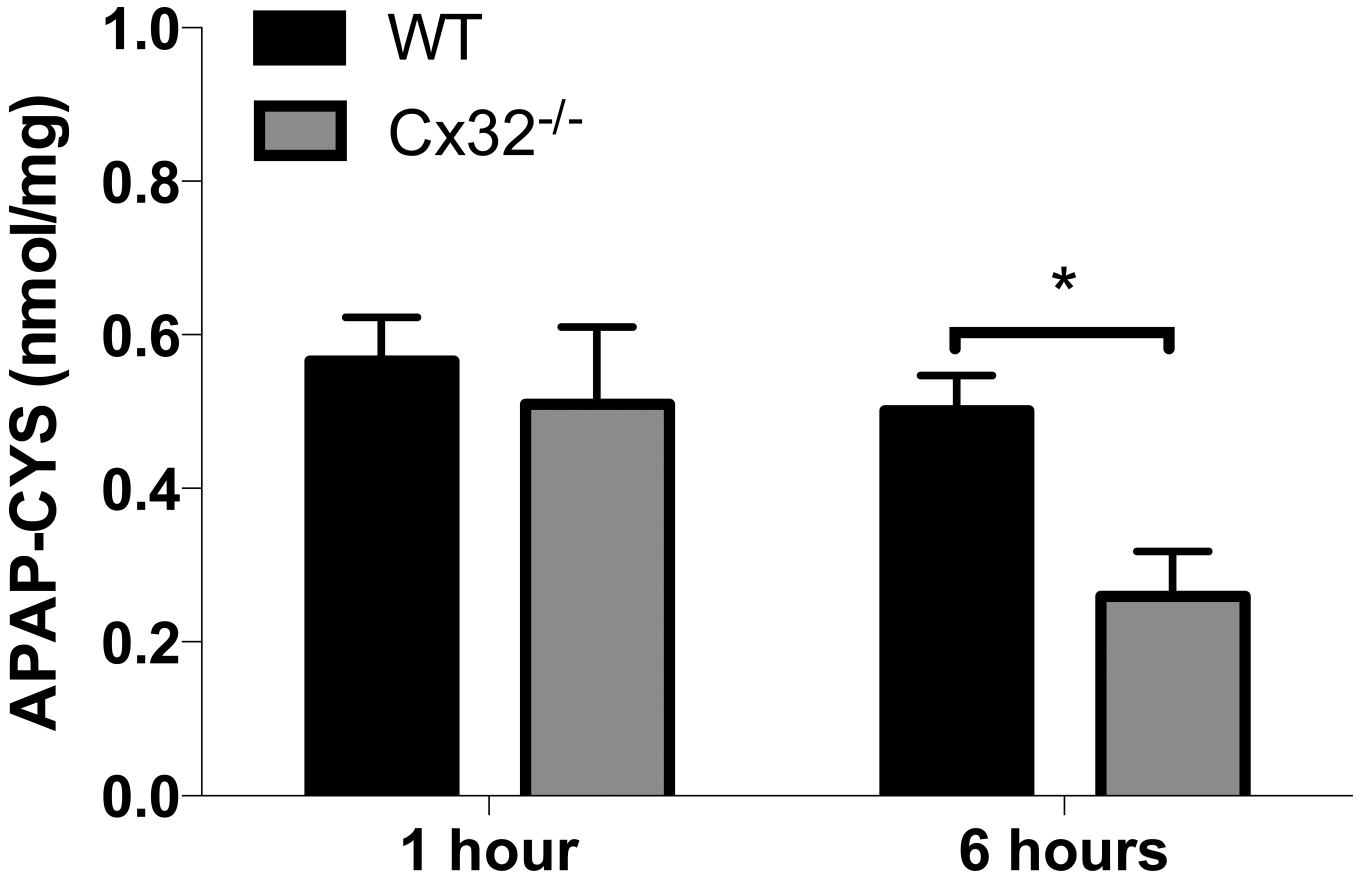

Figure 2. Effects of Cx32 ablation on APAP protein adduct formation

WT and Cx32$^{-/-}$ mice (n = 3-8) were overdosed with 300 mg/kg APAP followed by sampling after 1 hour and 6 hours. The generation of reactive metabolite results in the formation of APAP-CYS protein adducts, which were quantified by high-pressure liquid chromatography with electrochemical detection using total liver homogenate. Results were evaluated by 1-way ANOVA followed by *post hoc* tests using Bonferroni correction. Data were expressed as means ± SEM with asterisks indicating significant differences (*$p \leq 0.05$) compared to WT animals at indicated time points.

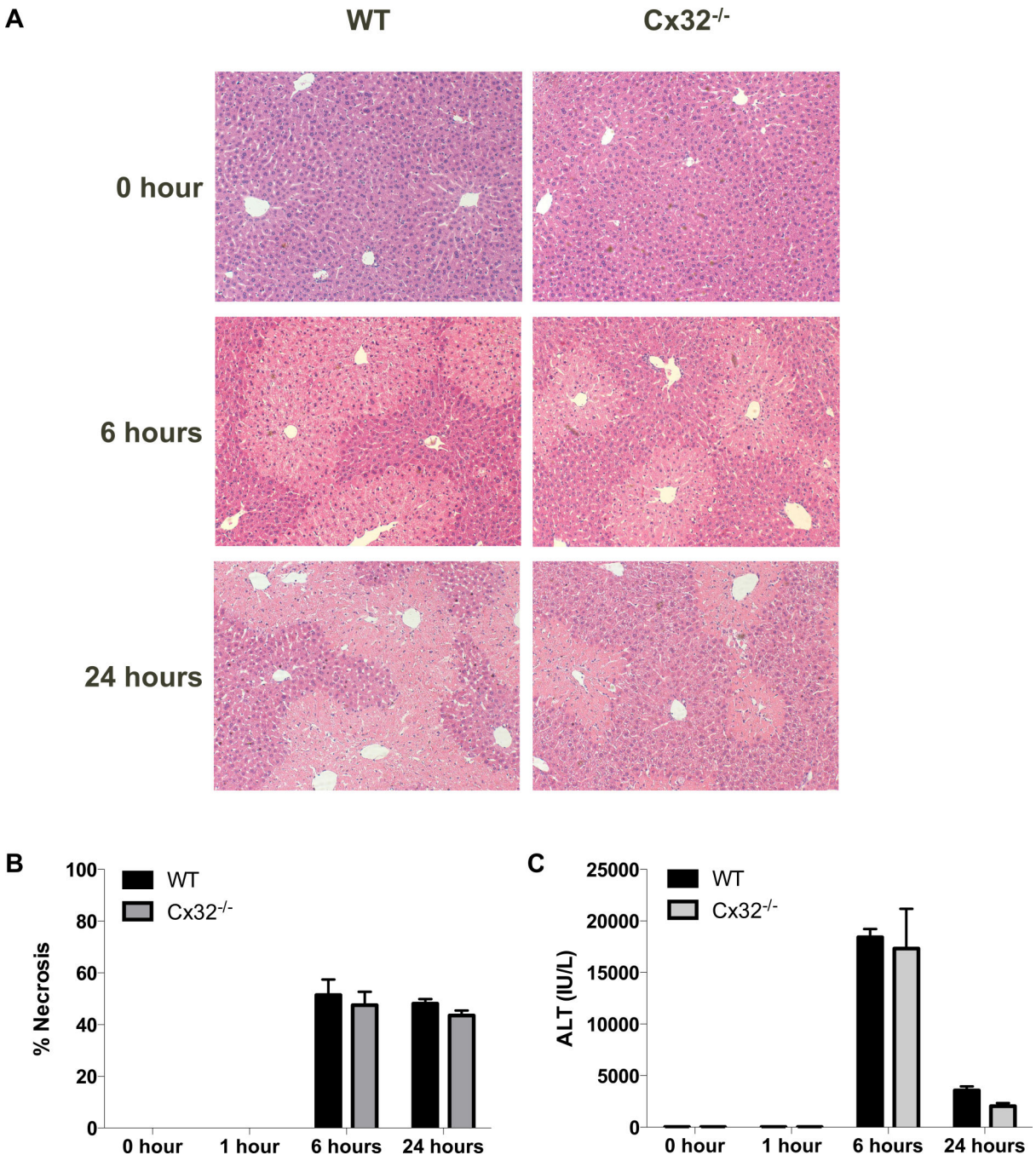

Figure 3. Effects of Cx32 ablation on APAP-induced liver cell injury

WT and $Cx32^{-/-}$ (n = 5-10) were overdosed with 300 mg/kg APAP followed by sampling at different time points. **(A)** Liver sections were examined microscopically at 100x magnification with **(B)** quantification of necrotic areas, typically located around the central vein. **(C)** Serum levels of ALT were measured at indicated time points. Results were evaluated by 1-way ANOVA followed by *post hoc* tests using Bonferroni correction. Data were expressed as means ± SEM. No statistically significant differences were found between $Cx32^{-/-}$ and WT animals.

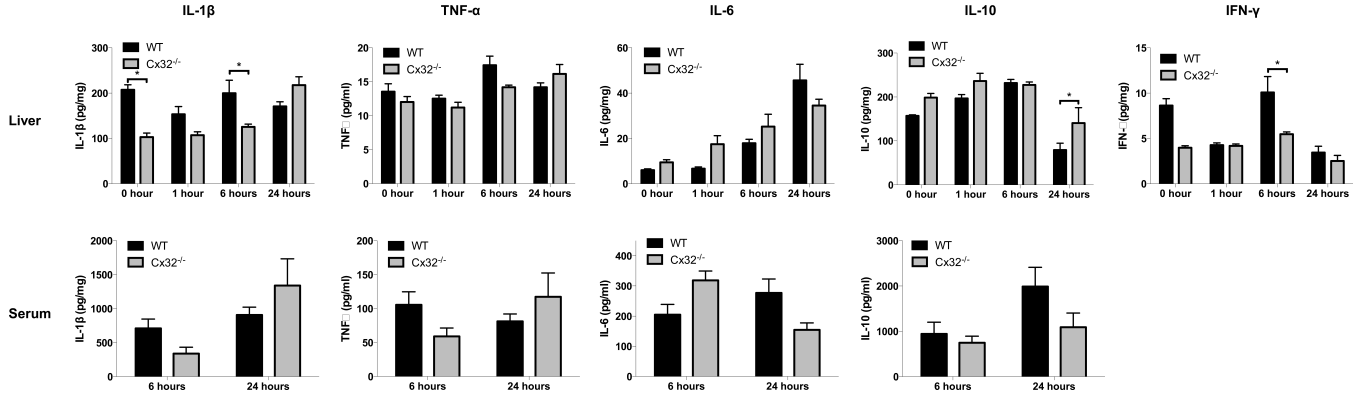

Figure 4. Effects of Cx32 ablation on APAP-induced inflammation

WT and Cx32$^{-/-}$ mice (n = 5-10) were overdosed with 300 mg/kg APAP followed by sampling at different time points. ELISA analysis of IL-1β, IL-6, IL-10, IFNγ and TNFα were performed in liver (upper panels) and serum (lower panels) samples. Results were evaluated by 1-way ANOVA followed by *post hoc* tests using Bonferroni correction. Data were expressed as means ± SEM with asterisks indicating significant differences ($*p \leq 0.05$) compared to WT animals at indicated time points.

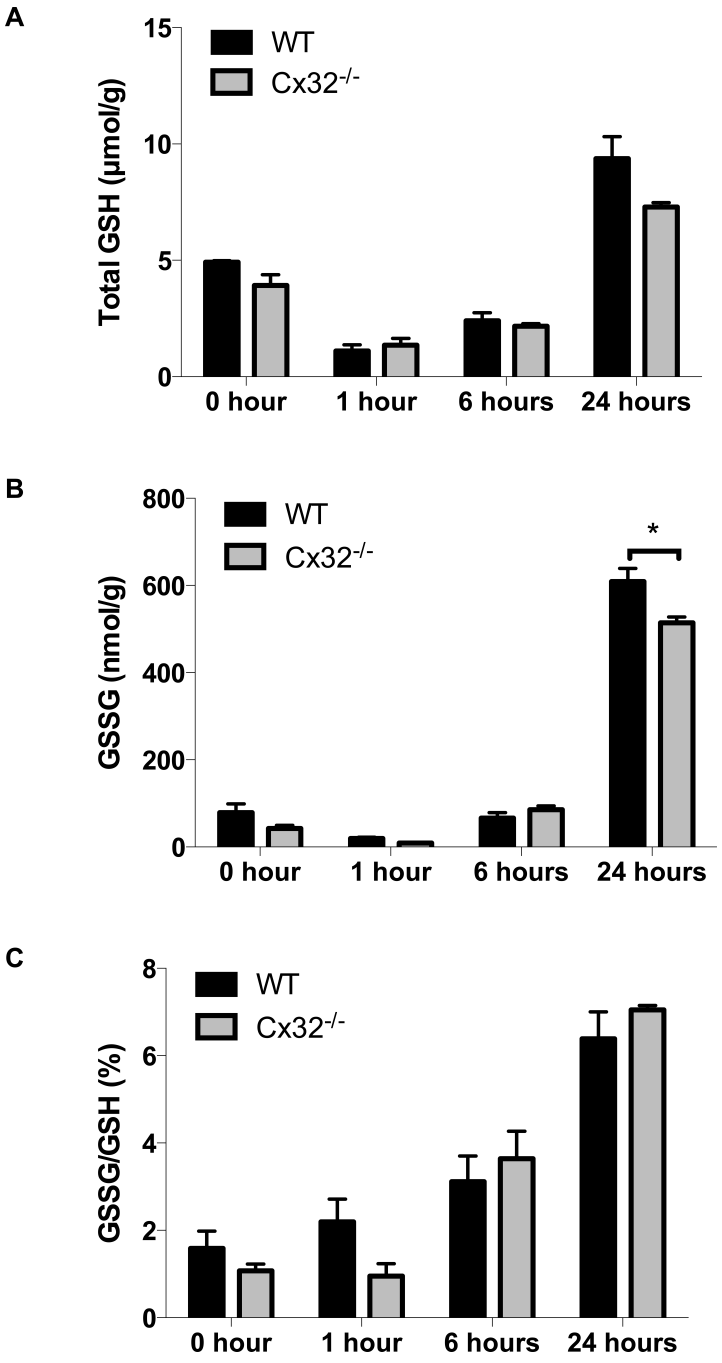

Figure 5. Effects of Cx32 ablation on APAP-induced oxidative stress

WT and $Cx32^{-/-}$ mice (n = 3-10) were overdosed with 300 mg/kg APAP followed by sampling at different time points. Hepatic levels of **(A)** GSH and **(B)** GSSG were measured in liver and **(C)** the GSSG/GSH ratio was calculated. Results were evaluated by 1-way ANOVA followed by *post hoc* tests using Bonferroni correction. Data were expressed as means ± SEM with asterisks indicating significant differences ($*p \leq 0.05$) compared to WT animals at indicated time points.

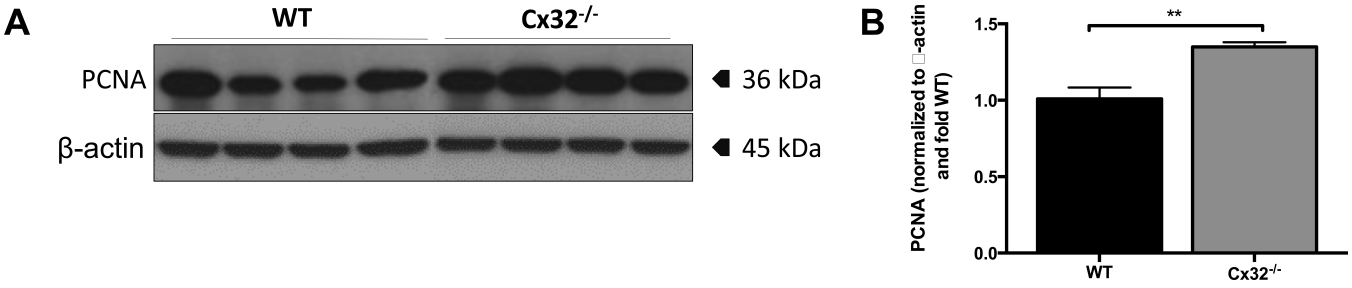

Figure 6. Effects of Cx32 ablation on APAP-induced hepatic regeneration

WT and $Cx32^{-/-}$ mice (n = 4-10) were overdosed with 300 mg/kg APAP followed by sampling after 24 hours. **(A)** Hepatic protein levels of PCNA and β-actin were assessed by immunoblot analysis. **(B)** Semi-quantitative densitometric analyses of PCNA were normalized against β-actin. Results were evaluated by 2-tailed unpaired student *t*-tests and Welch's correction. Data were expressed as means ± SEM with asterisks indicating significant differences (**$p \leq 0.01$) compared to WT animals.